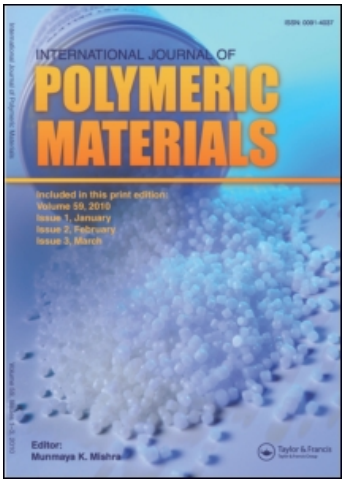

International Journal of Polymeric Materials
Publication details, including instructions for authors and subscription information:
http://www.informaworld.com/smpp/title~content=t713647664

Dielectric and Ion Transport Studies in [PVA: $LiC_2H_3O_2$]: $Li_2Fe_5O_8$ Polymer Nanocomposite Electrolyte System

S. L. Agrawal[a]; Markandey Singh[ab]; Nidhi Asthana[b]; Mrigank Mauli Dwivedi[b]; Kamlesh Pandey[b]
[a] Department of Physics, A.P.S. University, Rewa, (M.P.), India [b] National Centre of Experimental Mineralogy and Petrology, University of Allahabad, Allahabad, (U.P.), India

Online publication date: 04 January 2011

To cite this Article Agrawal, S. L. , Singh, Markandey , Asthana, Nidhi , Dwivedi, Mrigank Mauli and Pandey, Kamlesh(2011) 'Dielectric and Ion Transport Studies in [PVA: $LiC_2H_3O_2$]: $Li_2Fe_5O_8$ Polymer Nanocomposite Electrolyte System', International Journal of Polymeric Materials, 60: 4, 276 — 289
To link to this Article: DOI: 10.1080/00914037.2010.504178
URL: http://dx.doi.org/10.1080/00914037.2010.504178

International Journal of Polymeric Materials, 60:276–289, 2011

ISSN: 0091-4037 print/1563-535X online
DOI: 10.1080/00914037.2010.504178

Taylor & Francis
Taylor & Francis Group

Dielectric and Ion Transport Studies in (PVA: $LiC_2H_3O_2$): $Li_2Fe_5O_8$ Polymer Nanocomposite Electrolyte System

S. L. Agrawal,[1] Markandey Singh,[1,2] Nidhi Asthana,[2] Mrigank Mauli Dwivedi,[2] and Kamlesh Pandey[2]

[1]Department of Physics, A.P.S. University, Rewa (M.P.), India
[2]National Centre of Experimental Mineralogy and Petrology, University of Allahabad, Allahabad (U.P.), India

The present work deals with the findings on optical and ion transport behavior in a ferrite-doped polymer nanocomposite electrolyte system, namely, $[(100-x)\ PVA + xLiC_2H_3O_2]$: $yLiFe_5O_8$. This polymer electrolyte system has been characterized by SEM, DSC, IR and C-V measurements. The addition of filler seems to disturb the crystalline nature of the host matrix while the doping of salt shows a similar structure, but with a separate entity in SEM images. DSC studies reflect the interaction of the salt/filler with polymer with a change in morphology of the composite system. These results are well-corroborated by IR data. The effect of salt or filler in the enhancement of the a.c. conductivity of nanocomposite polymer electrolyte (NCPE) as well as dielectric relaxation behavior has been investigated with the help of impedance spectroscopy data. The a.c. conductivity of nanocomposite polymer electrolytes is seen to be best described by the universal power law.

Keywords DSC, impedance studies, polymer nanocomposite electrolyte, protonic and lithium ion conduction

Received 14 April 2010; accepted 16 June 2010.
The author (KP) is thankful to the Council of Science & Technology U.P. India for the financial support of this work.
Address correspondence to Kamlesh Pandey, N.C.E.M.P. 14 Chathum Line, Bank Road, University of Allahabad, Allahabad 211002, India. E-mail: kp542831@gmax.com

INTRODUCTION

Recently, solid composite polymer electrolytes have emerged as potential candidates for various electrochemical devices such as high performance batteries, fuel cells, super capacitors, sensors, and smart windows, on account of the possibility of achieving high ionic conductivity, and better mechanical and thermal stability [1–3]. The ability to form proper electrode-electrolyte contacts and ease of fabrication in desirable sizes has provided impetus to polymer electrolytes in comparison to other electrolyte system. Within this framework, polyvinyl alcohol (PVA)-based polymer electrolytes using alkali salts, plasticizers and inorganic/organic fillers have been extensively studied in the recent past [4–6]. PVA is a semicrystalline, water-soluble polymer with 1,3,glycol structure [7]. In PVA-based electrolytes, it has been shown that anion / cation mobility is confined in the amorphous phase and conduction occurs through a complex mechanism involving PVA segmental mobility. Heterogeneous doping of ferrite/inorganic/organic fillers leading to the formation of composites is one of the effective methods to improve the conductivity of these polymer electrolytes [8–9]. Addition of ferrite filler in the PVA matrix is likely to enhance the polar characteristics of the polymer, making it electrically more conductive. In this system, filler may reside at various sites. It may substitute on the polymer chain at the amorphous or crystalline boundaries and preferentially into the amorphous regions of the polymer. In recent times, ferrite nanoparticles have shown their worth in magnetic drug targeting, tissue engineering, DNA isolation, magnetic resonance imaging contrast agents and hyperthermia [10–11]. Besides, it has been asserted that the addition of ferrite creates additional hopping sites for the charge carriers and hence increases its concentration to result in an increase of conductivity [12]. With these perspectives in mind, the electrical behavior of PVA-based polymer nanocomposite electrolyte was evaluated from impedance spectroscopic technique. IR, SEM, DSC and CV data were also recorded and analyzed to support the electrical response.

EXPERIMENTAL

Polyvinyl alcohol (PVA) based nanocomposite electrolyte films were prepared by solution cast technique. Lithium acetate ($LiC_2H_3O_2 \cdot 2H_2O$) salt dissolved in D.I. water was admixed in proper stiochiometric composition in the polymer to form a pristine polymer electrolyte. Ferrite powder ($Li_2Fe_5O_8$) was synthesized by the standard sol-gel technique. Lithium nitrate and iron nitrate were chosen as precursor materials dissolved in a double-distilled water/ethanol mixture for the formation of lithium ferrite powder. The sol with pH ranging in between 2–3 was allowed to gel at 50°C. The gel was dried at 150°C for 12 h

followed by thermal treatment at 700°C (for 2 h) and 900°C (for 0.5 h) in a kenthal high temperature furnace. The dried material was crushed to obtain fine powder of lithium ferrite. Finally the powder was annealed up to 900°C to order cation distribution in ferrite [13]. This powder was dispersed in a pristine electrolyte solution followed by magnetic stirring for a prolonged period of time at an elevated temperature. Solution-cast film was dried at constant 30°C in BOD incubator.

The thermal behavior of different polymeric systems was studied by differential scanning calorimetry (DSC, instrument model: Netzsch 200 F3) in the temperature range 25°C–150°C with the heating rate of 5°C/min under N_2 ambient. The SEM image of different composite electrolytes was recorded with the help of a Jeol JXA-8100 EPMA instrument.

C-V measurements on electrolyte film were performed on a CH-electrochemical workstation, model 608. The IR spectra were recorded on a Perkin Elmer spectrometer in the range 500–4000 cm^{-1}. Electrical characterization of the electrolyte was carried out using impedance spectroscopy technique. The complex impedance parameters were measured with a Hioki (model 3520) impedance analyzer in the frequency range 40 Hz−100KHz using platinum electrodes for electrical contact.

RESULTS AND DISCUSSION

Figure 1 shows the thermograms of PVA, 80PVA:20$LiC_2H_3O_2$ electrolyte film and [80PVA:20$LiC_2H_3O_2$]:5% $Li_2Fe_5O_8$ composite polymer electrolyte film. In

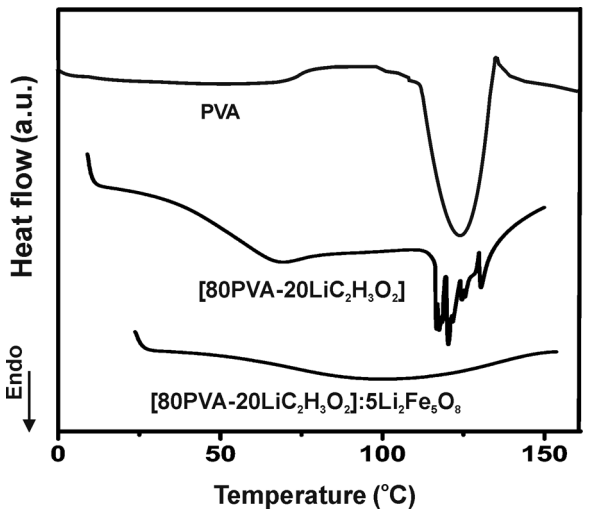

Figure 1: DSC pattern of PVA, PVA + $LiC_2H_3O_2$ and (PVA + $LiC_2H_3O_2$): $Li_2Fe_5O_8$ polymer composite electrolytes.

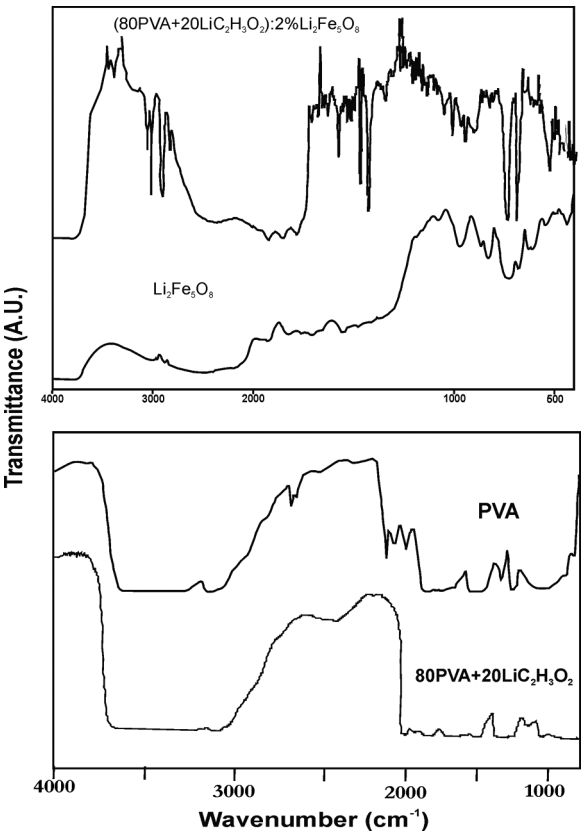

Figure 2: Infrared spectrum of PVA, PVA + $LiC_2H_3O_2$ and (PVA + $LiC_2H_3O_2$): $Li_2Fe_5O_8$ polymer composite electrolytes.

the DSC study of pure PVA film, an endothermic peak was observed at 125°C while T_g of polymer was apparent around 75°C. Endothermic transition around 125°C is attributed to T_{t1} for PVA. This transition in PVA is obtained due to easy detachment of small molecules of bound water from the texture leading to a higher change in the value of entropy. This behavior of PVA has also been explained as Phenton melting. This transition is essentially not due to the melting of polymer, but rather related to some kind of sol-gel transition [14].

In a pristine polymer electrolyte, the glass transition temperature shifts towards the lower temperature range and a broad endothermic peak correlated to the complete dehydration of $LiC_2H_3O_2 \cdot 2H_2O$ [15] appears at 64°C. The peak at 125°C in PVA splits into multiple peaks after complexation as a result of the interaction of PVA with $LiC_2H_3O_2$ salt (formation of acetic acid with the release of extra water). The combined effect of $LiC_2H_3O_2 \cdot 2H_2O$ and $Li_2Fe_5O_8$ was observed on the thermal behavior of NCPE, causing an

extremely broad peak in the higher temperature range. The thermogram also reveals the partial amorphous nature of the nanocomposite electrolyte. The onset of this broad peak centered around 96°C starts from 78°C. In this region $Li_2Fe_5O_8$ shows a small weight loss in TGA records. This is due to the partial removal of hydrated water [16–17]. Improvement in the amorphous behavior of the electrolyte is reflected in the broadness of this transition.

Infrared spectra of pristine materials as well as NCPE are shown in Figure 2. A main feature of alcohols is the appearance of the OH (hydroxyl) vibrational band at 3589 cm^{-1} in the range of 3600–3400 cm^{-1}. These bands in PVA get displaced toward the lower wavenumber and appear as a broad hydroxyl band in the complex. The absorption band at 1726, 1410 and 1260 cm^{-1} are respectively assigned to C=O stretching of unhydrolyzed acetate portion, weak OH bending deformation and C-O bend deformation of PVA. These bands shift to 1715, 1417, 1259 and 926 cm^{-1} in the complex. The C-C stretching frequency of secondary alcohol of PVA at 1100 cm^{-1} is displaced to 1098 cm^{-1} in the complex. An asymmetric CH_2 stretching and CH bend of CH_2 vibrational frequencies (2954 and 1417 cm^{-1}) of PVA [18] were found to be absent in the complex. The observed stretching band at 1124 cm^{-1} either corresponds to the crystallization-sensitive band of PVA or it might be due to a kind of absorption mechanism related to the presence of the oxygen atom [19].

Formation of the spinel phase is revealed in the IR spectra of lithium ferrite through exhibition of two IR fundamental frequencies at ν_1 (630–560 cm^{-1}) and ν_2 (525 cm^{-1}). The ν_1 band may be attributed to vibrations of the octahedral phase and ν_2 to complex vibration involving both octahedral and tetrahedral sites. The IR peaks at 590 and 550 cm^{-1} with shoulders at 700 and 680 cm^{-1} substantiate formation of the "ordered" spinelic phase [20]. The addition of salt/filler in NCPE generates a few new absorption peaks, giving an indication of complex formation. Peaks at 1590, 1430, 1220 and 1020 cm^{-1} are indicative of the formation of new metal acetate in the NCP electrolyte [21]. Increase in intensity of the peaks in the region 3000 to 2500 cm^{-1} was observed after complexation which is linked to the basic acetates in the presence of PVA. This substantiates the complexation of salt/filler with the polymer matrix.

Figure 3 shows the SEM image of composite electrolyte with different ferrite content viz. [80PVA-20$LiC_2H_3O_2$]: x% $Li_2Fe_5O_8$, (where x = 0.5, 2, 5, and 10). The SEM images reveal surface morphology and evidence of the heterogeneous phase in the nanocomposite electrolyte system. Addition of Li-ferrite filler in the electrolyte (80PVA-20 $LiC_2H_3O_2$) system is seen to break the original structure of pure PVA and disturb the crystalline nature of the original matrix. Particle size obtained by SEM is ~50–60 nm for system with 2% Li-ferrite filler content. Though the amount of filler in excess of 5% shows segregation in the matrix, a further increase in ferrite content changes the morphology of the composite system.

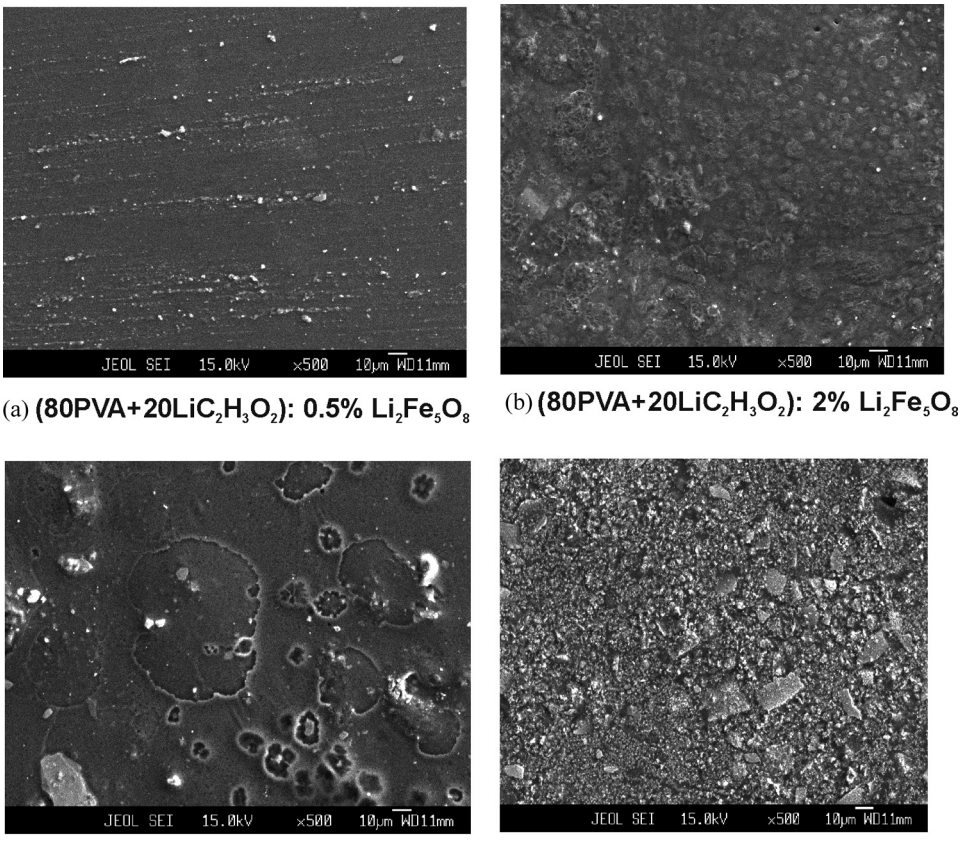

(a) **(80PVA+20$LiC_2H_3O_2$): 0.5% $Li_2Fe_5O_8$** (b) **(80PVA+20$LiC_2H_3O_2$): 2% $Li_2Fe_5O_8$**

(c) **(80PVA+20$LiC_2H_3O_2$): 5% $Li_2Fe_5O_8$** (d) **(80PVA+20$LiC_2H_3O_2$): 10%$Li_2Fe_5O_8$**

Figure 3: SEM image of different NCPE systems.

Figure 4 shows the variation of conductivity with lithium ferrite filler concentration. The bulk electrical conductivity increases with increasing ferrite filler till 2 wt% before decreasing (up to 5 wt%) and finally shooting up again. This result clearly shows a behavior best described by the double percolation model for bulk electrical conductivity, proposed by Chandra and coworkers [22] for composite electrolytes. These two peaks probably arise due to mobility of two cationic species (i.e., H^+ and Li^+) [23]. The DSC and IR results also indicate the formation of an intermediate phase like acetic acid, which acts as a possible supplier of protons, giving rise to concentration of carriers and thus the conductivity of electrolyte. Similarly, salt/filler provide the Li^+ for conduction. Detailed analysis is underway.

In the present study, the likely mobile species are protonic and lithium ion. Thus, thick platinum electrodes were used in amperometric I-t technique to

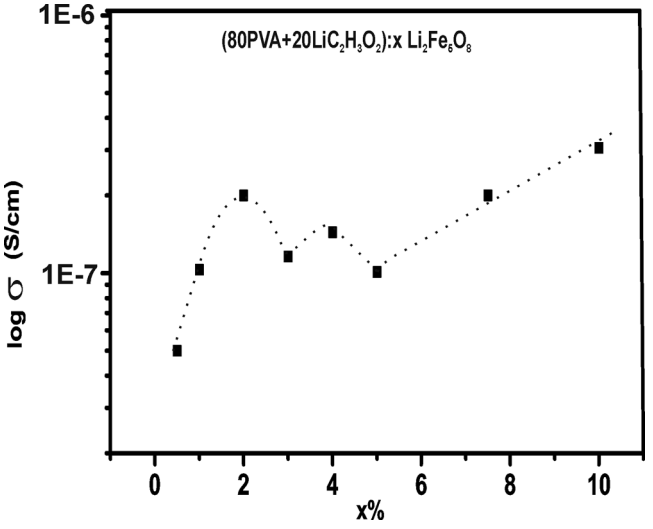

Figure 4: Variation of bulk conductivity with different composition of Li-ferrite.

assess the nature of ion transport and evaluate total ionic transference number from the current time plot. The variation of current with time for one of the NCPE, i.e., [80 PVA: 20 $LiC_2H_3O_2$]: 2% $Li_2Fe_5O_{8,}$ is given in Figure 5. From these plots the initial current $i_{initial}$ and final current i_{final} was noted and the total ionic transference number (t_{ion}) was calculated using the relation

$$t_{ion} = \frac{i_{initial} - i_{final}}{i_{initial}} \quad (1)$$

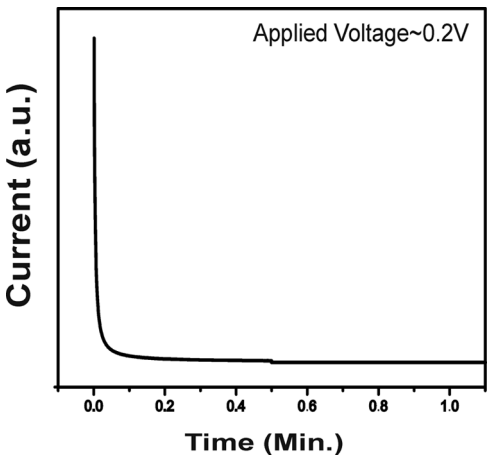

Figure 5: Variation of current with time for (80PVA + 20$LiC_2H_3O_2$): 2% $Li_2Fe_5O_8$ system.

The calculated values of t_{ion} for different composite films are in excess of 0.9, which ascertains ionic charge transport in a composite system. These values are at best qualitative due to (a) nonavailability of the ideal blocking electrode for protonic/gaseous species, and (b) uncertainty in the measurement of the initial current due to quick onset of polarization.

The electrochemical stability window is essential information for the success of any device, and particularly in energy storage devices. Figure 6 represents the cyclic voltammogram of [80PVA:20$LiC_2H_3O_2$]:2% $Li_2Fe_5O_8$ composite polymer electrolyte. The cyclic voltammetry has been performed for the Pt/composite polymer electrolyte/Pt cell with a scan rate 0.1 volt/sec for five cycles to affirm excellent reversibility of electrolytes. The following inference has been drawn from the cyclic voltammogram. The electrochemical window has been obtained as -3.0 to $+3.0$ volt for [80PVA:20$LiC_2H_3O_2$]:2% $Li_2Fe_5O_8$ composite polymer electrolyte. Small cathodic and anodic peaks were also observed. These peaks may be due to the interaction of iron and lithium in polymer electrolyte as also evidenced during the IR studies.

The variation of a.c. conductivity with frequency and lithium ferrite filler content is shown in Figure 7. The a.c. conductivity of the composite polymer electrolytes increases with increasing frequency. The a.c. conductivity (σ_{ac}) of the sample seems to follow the well-known universal power law [24]:

$$\sigma_{ac} = A\omega^n \tag{2}$$

where, A is the pre-exponential factor and n the fraction exponent lying between 0 and 1. The calculated value of n for the best conducting [80PVA:20$LiC_2H_3O_2$]:2% $Li_2Fe_5O_8$ composite polymer electrolyte is $\sim$0.9.

Figure 8(a) shows the temperature-dependent behavior of bulk conductivity, and Figure 8(b) shows the variation of a.c. conductivity with frequency

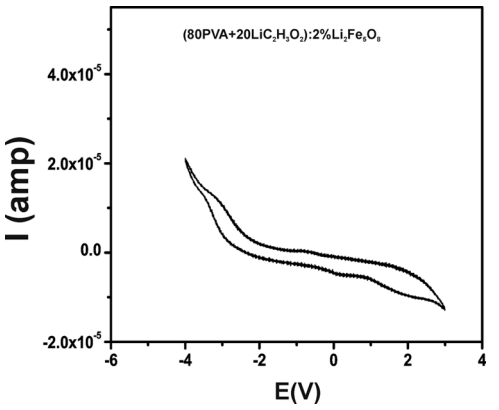

Figure 6: Variation of current with applied potential for (80PVA + 20$LiC_2H_3O_2$): 2% $Li_2Fe_5O_8$ system.

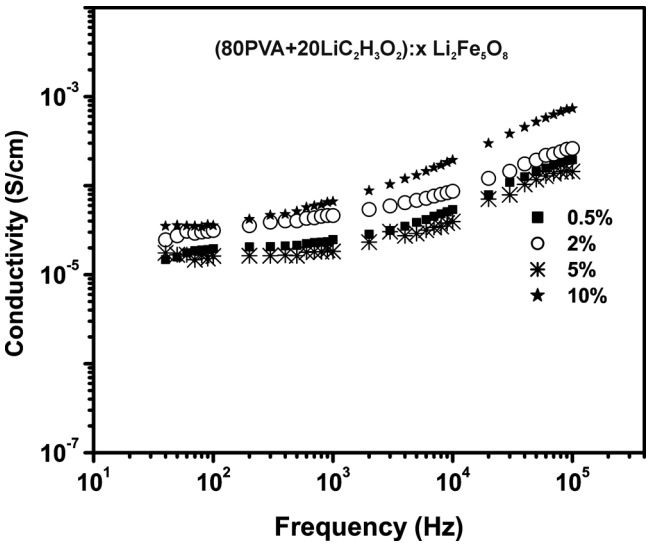

Figure 7: Variation of a.c. conductivity with frequency for different composition of Li-ferrite.

at different temperatures for [80PVA-20$LiC_2H_3O_2$]:2% $Li_2Fe_5O_8$ composite electrolyte. The bulk electrical conductivity increases with increasing temperature up to 60°C with a change in slope thereafter till 78°C. The log σ vs. 1/T plot shows the combination of Arrhenius and VTF behavior described as under

$$\sigma = \sigma_0 exp(-E_a/KT) \tag{3}$$

and

$$\sigma = \sigma_0 T^{-1/2} exp(-E_a/T - T_0) \tag{4}$$

where, E_a is the activation energy and K the Boltzmann constant.

The addition of ferrite fillers tries to enhance the conductivity value with temperature due to its interaction with components as evidenced in IR studies. Interestingly beyond 78°C, conductivity decreases due to an increase in crystallinity (obtained in DSC measurements). In the same temperature range the magnetization of the Li ferrite also decreases with temperature rapidly [25], which might be another factor for the decrease in conductivity of the composite electrolyte system. Similar behavior is noticed in the a.c. conductivity response of NCPE.

Figures 9(a) and 9(c) show the variation of dielectric constant (ε') and dielectric loss (ε'') as a function of frequency for different synthesized nanocomposite polymer electrolytes. Strong frequency dispersion in dielectric

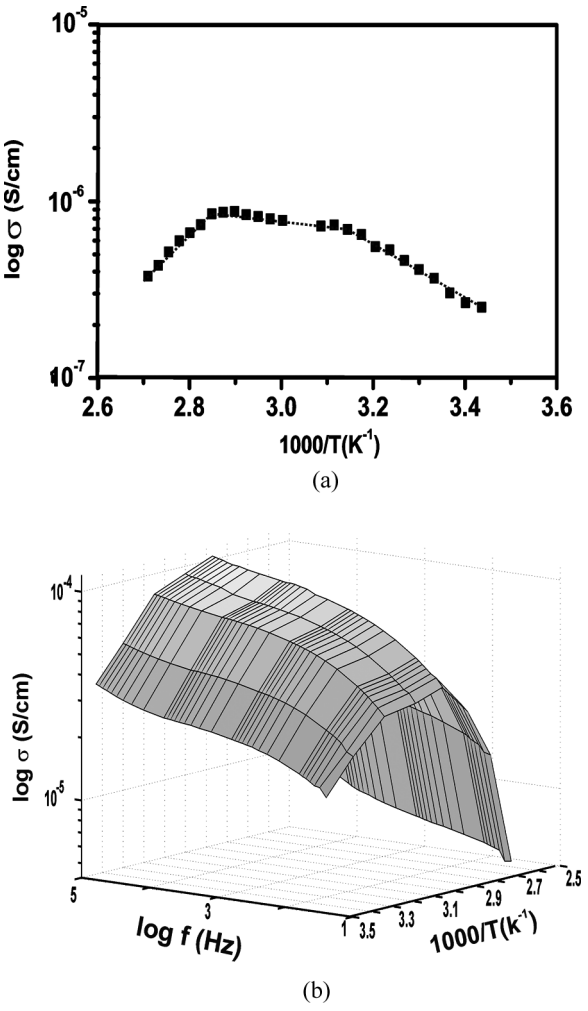

Figure 8: Variation of conductivity with temperature (a) by Cole-Cole plot and (b) at different frequencies for (80PVA + 20$LiC_2H_3O_2$): 2% $Li_2Fe_5O_8$ polymer composite electrolytes.

constant and dielectric loss was recorded in the lower frequency region followed by frequency-independent behavior at higher frequencies (above 10 KHz). The decrease in ε' and ε'' with frequency is attributed to electrical relaxation or inability of dipole to rotate rapidly to follow the applied field. In a low-frequency region, ion aggregation at interface leads to a net polarization which allows formation of the space charge region at electrode–electrolyte interface. As the frequency increases, the ionic and orientational source of polarizability decreases and finally disappears due to inertia of the mobile ions, thereby causing a constant value of dielectric constant. It also shows the non-Debye type nature of the electrolyte system. With salt content the increase in dielectric loss

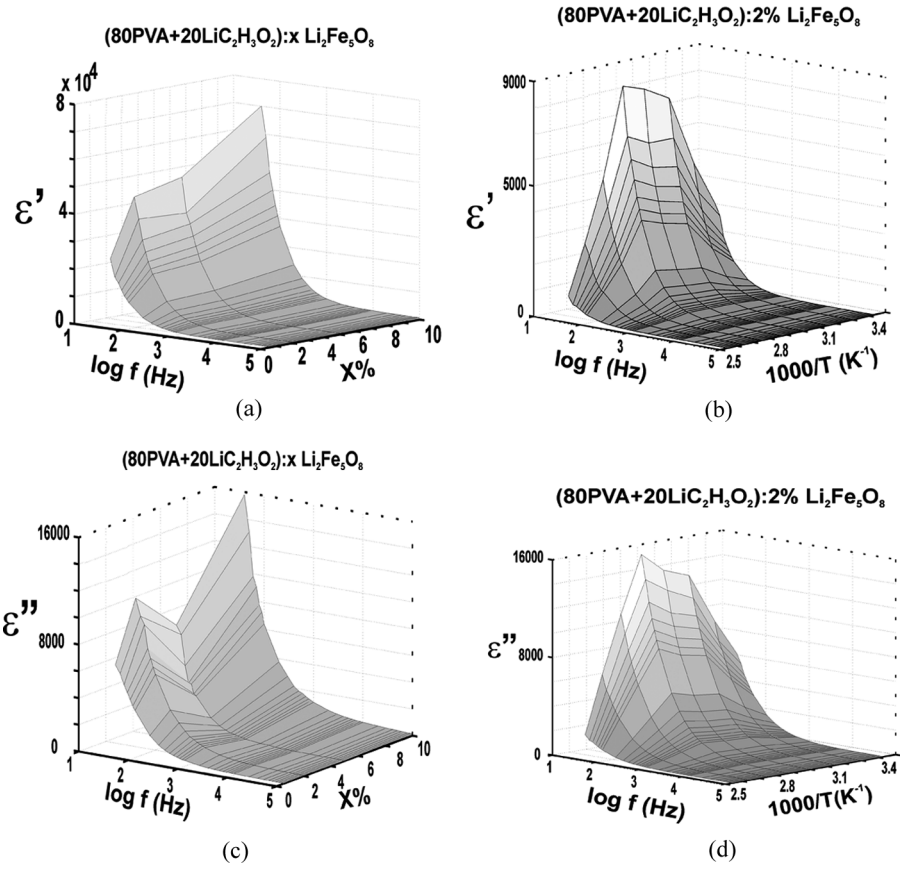

Figure 9: Variation of different dielectric parameters with frequency and temperature.

value is possibly due to extra free charge carriers provided by the salt and ferrite filler.

In Figures 9(b) and 9(d), the variation of dielectric constant (ε') and dielectric loss (ε'') as a function of frequency at different temperatures of [80PVA:20$LiC_2H_3O_2$]:2% $Li_2Fe_5O_8$ composite polymer electrolyte is shown. Both ε' and ε'' seem to increase till 78°C before sharply decreasing. The increase in dielectric constant/dielectric loss is possibly on account of thermally activated charge carriers, while the decrease in these values is on account of the magnetization of $Li_2Fe_5O_8$[26], which has been reported to diminish at high temperature. Another possibility for this decrease is enhancement of crystallinity beyond 78°C in the NCPE (evidenced from DSC measurements). The tangent loss ($\tan\delta$) variation with frequency for different compositions is shown in Figure 10(a). The maximum tangent loss was observed in 2% $Li_2Fe_5O_8$-based system. The higher value of tangent loss can be attributed to segmental diffusion motion in the amorphous region which

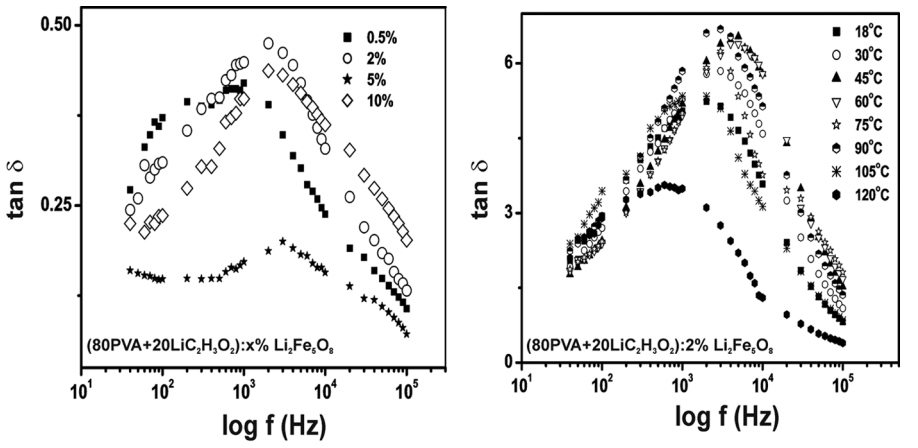

Figure 10: Variation of tan loss with (a) frequency and (b) temperature for polymeric system.

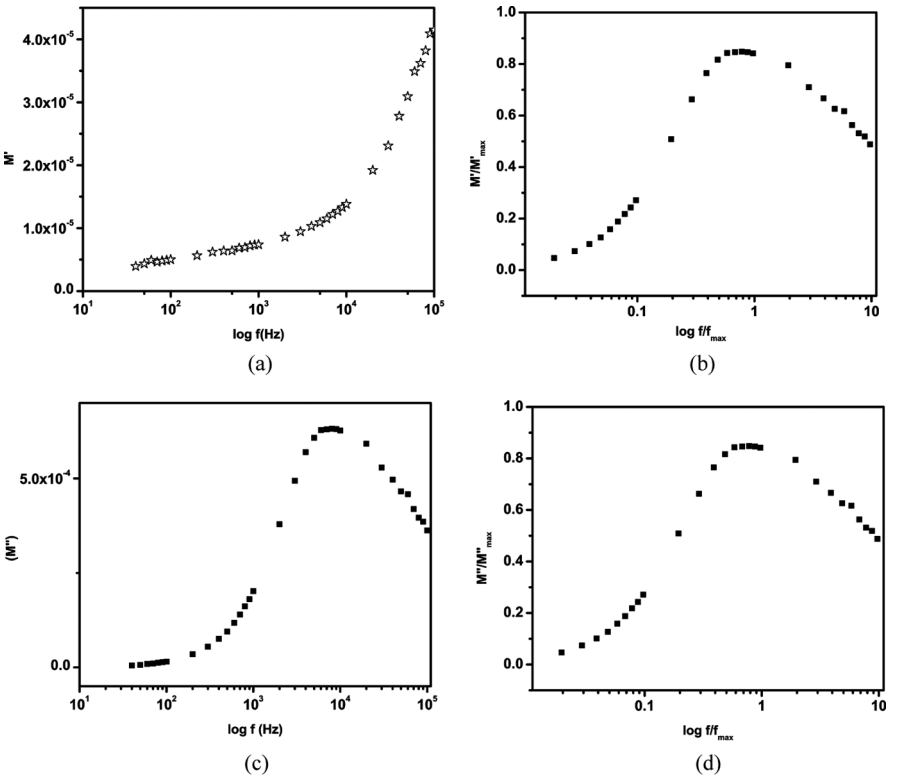

Figure 11: Variation of real and imaginary part of mod. of electricity with frequency for (80PVA + 20$LiC_2H_3O_2$): 2% $Li_2Fe_5O_8$ system.

enhances (DSC studies) for 2 wt% filler in NCPE. Interestingly, closer examination of this figure reveals two tanδ peaks (one peak and a shoulder) both of which shift to higher frequencies with temperature but shift to lower frequencies for higher filler contents. This feature is probably on account of the interaction of lithium and its attachment to the side chain, making it difficult to follow high frequencies. Figure 10(b) shows the temperature-dependent behavior of tangent loss for the [80PVA:20$LiC_2H_3O_2$]:2% $Li_2Fe_5O_8$ system. Here we observe that the tangent peak shifts towards the lower frequency side with increasing temperature on account of the chiotic motion of mobile species. It is interesting to note that relaxation peaks are askewed at higher temperatures, probably on account of the different relaxation times of mobile species (Li^+ and H^+/OH^-).

To reduce the effect of electrode polarization, Macedo et al. [27] have introduced the electric modulus $M^*(=1/\varepsilon^*)$ formalism. For the given temperature and frequency, the real part M′ and the imaginary part, M″ of complex modulus were extracted from impedance data.

The frequency dependence of M′, M″ and normalized behavior for different electrolytes are shown in Figure 11. The normalized behavior of the modulus shows that interfacial polarization completely vanishes above 1 KHz frequency. The peak in normalized M″ can be related to translational ion dynamics and mirrors the conductivity relaxation of the mobile ions.

CONCLUSION

Different experimental tools, i.e., SEM, IR, and electrical conductivity, show the physical and morphological behavior of nanosized Li-ferrite doped PVA nanocomposite electrolyte. SEM observations confirm the formation of a nanocomposite system with crystallite size varying between 5–60 nm. The electrical conductivity is enhanced by ~3–4 orders upon dispersion of Li-ferrite and also shows the Arrhenius-VTF combined nature of the electrolyte. The C-V studies show a wide electrochemical window for device applications.

REFERENCES

[1] Koo, J. H. (2006). *Polymer Nanocomposites: Processing, Characterization, and Applications*, McGraw-Hill, New York.

[2] Agrawal, R. C., and Pandey, G. P. *J Phys. D: App. Phys*. **41**, 223001 (2008).

[3] Pandey, K., Dwivedi, M. M., Singh, M., and Agrawal, S. L. *J. Polymer Research*. **17**, 127 (2010).

[4] Agrawal, G. S., and Dutta Gupta, S. *Phys. Rev. A* **57**, 667 (1997).

[5] Mehendru, P. C., Pathak, K., Jain, K., and Mehendru, P. *Phys. Stat. Sol.* **1**, 403 (1997).

[6] Agrawal, S. L., and Awadhia, A. *Bull. Mater. Sci.* **27**, 523 (2004).

[7] Ranby, B., and Rabak, J. F. (1977). *ESR Spectroscopy in Polymer Research*, Springer, New York.

[8] Kang, B., and Wu, J. W. *Journal of Korean Physical Society.* 49, 955 (2006).

[9] Agrawal, S. L., and Shukla, P. K. *Ionics.* **6**, 312 (2000).

[10] Mostafa, A. A., El-Shobaky, G. A., and Girgis, E. *J. Phys. D: Appl. Phys.* **39**, 2007(2006).

[11] Gangopadhyay, S., Hadjipanayis, G. C., Dale, B., Sorenson, C. M., Klabunde, K. J., Papaefthymiou, V., and Kostikas, A. *Phys. Rev. B* **45**, 9778 (1992).

[12] Yavuz, O., Ram, M. K., Aldissi, M., Poddar, P., and Hariharan, S. *J. Mat. Chem.* **15**, 810 (2005).

[13] Jovic, N. G., et al. *J. Phys. Chem. C* **113**, 20559 (2009).

[14] Mukherjee, G. S., Shukla, N., Singh, R. K., and Mathur, G. N. *J. Scientific and Industrial Research.* **63**, 596 (2004).

[15] Baijal, J. S., Phanjoubam, S., and Kothari, D. *Solid State Comm.* **83**, 679 (1992).

[16] Kim, S. J., Park, S. T., Kim, I. Y., Lee, Y. H., and Kim, S. I. *J. Applied Polymer Science.* **869**, 1844 (2002).

[17] Lagashetty, A. K., Habanoor, V., Basawaraja, S., and Venkatraman, A. *Bull. Mater Sci.* **28**, 477 (2005).

[18] Rajendran, S., Sivkumar, M., Subadevi, R., Wu, N.-L., and Lee, J.-Y. *J. Appl. Polymer Science.* **103**, 3950 (2007).

[19] Elliot, A., Ambrose, E. J., and Temple, R. B. *J. Chem. Phys.* **16**, 877 (1948).

[20] Gingasu, D., Mindru, I., Patron, L., and Toleriu, S. S. *J. Serb. Chem. Soc.* **73**, 979 (2008).

[21] Jewur, S. S., and Kuriacose, J. C. *Thermochemica Acta.* **19**, 195 (1977).

[22] Chandra, A., Srivastava, P. C., and Chandra, S., *J.Mater. Sci.* **30**, 3633 (1995).

[23] Nasef, M. M., and Saidi, H. *Macromol. Mat. Engg.* **291**, 972 (2006).

[24] Jonscher, A. K. (1983). *Dielectric Relaxation in Solids*, Chelsea Dielectric Press, London, 310.

[25] Widatallah, H. M., Johnson, C., Berry, F., and Pekala, M. *Solid State Comm.* **120**, 171 (2001).

[26] Tabuchi, M., et al. *J. Solid State Chem.* **141**, 554 (1998).

[27] Macedo, P. B., Moynihan, C. T., and Bose, R. *J. Chem. Glasses.* **13**, 171 (1972).